Molecular Biology of the Cell
Vol. 5, 1105–1118, October 1994

Molecular Organization of Transverse Tubule/ Sarcoplasmic Reticulum Junctions During Development of Excitation-Contraction Coupling in Skeletal Muscle

Bernard E. Flucher,*† S. Brian Andrews,* and Mathew P. Daniels‡

*Laboratory of Neurobiology, National Institute of Neurological Disorders and Stroke; and
‡Laboratory of Biochemical Genetics, National Heart, Lung, and Blood Institute,
National Institutes of Health, Bethesda, Maryland 20892

Submitted June 10, 1994; Accepted August 15, 1994
Monitoring Editor: Roger Y. Tsien

The relationship between the molecular composition and organization of the triad junction and the development of excitation-contraction (E-C) coupling was investigated in cultured skeletal muscle. Action potential-induced calcium transients develop concomitantly with the first expression of the dihydropyridine receptor (DHPR) and the ryanodine receptor (RyR), which are colocalized in clusters from the time of their earliest appearance. These DHPR/RyR clusters correspond to junctional domains of the transverse tubules (T-tubules) and sarcoplasmic reticulum (SR), respectively. Thus, at first contact T-tubules and SR form molecularly and structurally specialized membrane domains that support E-C coupling. The earliest T-tubule/SR junctions show structural characteristics of mature triads but are diverse in conformation and typically are formed before the extensive development of myofibrils. Whereas the initial formation of T-tubule/SR junctions is independent of association with myofibrils, the reorganization into proper triads occurs as junctions become associated with the border between the A band and the I band of the sarcomere. This final step in triad formation manifests itself in an increased density and uniformity of junctions in the cytoplasm, which in turn results in increased calcium release and reuptake rates.

INTRODUCTION

Excitation-contraction (E-C) coupling is the signaling process in muscle by which membrane depolarization leads to force production (see Rüegg, 1988 for review). The second messenger in this process is calcium, which cycles between the sarcoplasmic reticulum (SR) and the cytoplasm. The terminal SR cisternae are specialized for storage and release of calcium, whereas longitudinal SR is the site of calcium uptake. Terminal cisternae form junctions with the plasma membrane, called peripheral couplings, or with transverse tubules (T-tubules), called triads. These junctions function in the coupling of membrane depolarization to calcium release.

The triads of mature striated muscle display a highly regular organization of their membrane compartments and their major molecular components. Furthermore, skeletal muscle triads are characterized by their regular orientation at specific locations in the sarcomere. A triad consists of a flattened portion of the T-tubule making junctions with terminal SR cisternae on both sides (Franzini-Armstrong, 1970). The 15-nm gap between the T-tubule and SR membranes is periodically spanned by electron dense structures called the "feet." These feet correspond to the large cytoplasmic domains of the SR calcium release channel, which is formed by a homotetramer of the ryanodine receptor (RyR) (Inui *et al.*, 1987; Lai *et al.*, 1988; Wagenknecht *et al.*, 1989). Junctional T-tubules are highly enriched in dihydropyridine receptors (DHPR) (Fosset *et al.*, 1983; Striessnig *et al.*, 1986; Jorgensen *et al.*, 1989; Flucher *et al.*, 1990). The primary function of this L-type calcium channel in skeletal muscle may be that of a voltage sensor in E-C coupling rather than conducting calcium (Rios and Brum,

† Corresponding author.

1987). Freeze-fracture of T-tubules shows the DHPR as groups of four integral membrane particles, called junctional tetrads (Block *et al.*, 1988). Their dimensions match the tetrameric structure of a foot, and their spacing corresponds to that of every other foot in the apposing SR membrane. Thus, a close interaction between the two channels has been suggested, which could be involved in the mechanical gating of the RyR in response to voltage-sensing of the DHPR.

These striking structural features of the triad are matched by equally striking functional properties of E-C coupling, including the speed at which cytoplasmic free calcium concentrations can be raised by several orders of magnitude and the synchrony of calcium release throughout the thickness of the muscle fiber (see Rüegg, 1988 for review). The structural organization of the triads and their regular distribution in the sarcomere may play a crucial role in the efficiency of the calcium release system. The reuptake of calcium into the SR is accomplished by the Ca^{2+}-ATPase that is highly enriched in a sheath of SR tubules surrounding the myofibrils (see Peachey and Franzini-Armstrong, 1983 for review). The efficiency of this system determines the speed of calcium removal from the cytoplasm that in turn determines the maximal rate of repetitive contraction-relaxation cycles. Although we are beginning to understand some of the structure-function relationships of the calcium release and reuptake system in skeletal muscle, little is known how these structures develop and how particular aspects of structural organization influence functions.

The structural development of the E-C coupling apparatus in skeletal muscle can be subdivided into three separate events: the molecular differentiation of the membrane compartments of T-tubules and SR, the formation of the junction between them, and the specific association of the membrane compartments with the myofibrils. Whereas the molecular composition of developing T-tubules is distinct from that of the plasma membrane, the latter shares the ability to form junctions with the SR during early development (Yuan *et al.*, 1990; Flucher *et al.*, 1991b). Junctional proteins may actually be inserted into the T-tubules by a separate pathway from nonjunctional T-tubule proteins (Yuan *et al.*, 1991). We have recently shown that the expression and clustering of the DHPR facilitates the structural differentiation of the E-C coupling membranes (Flucher *et al.*, 1991a, 1993a). However, the specialization of junctional SR can occur in the absence of the DHPR α_1 subunit in myotubes of the dysgenic mouse mutant. Furthermore, junctions with feet but without tetrads were observed in dysgenic muscle (Franzini-Armstrong *et al.*, 1991). Thus, junction formation appears to be independent of the molecular differentiation of at least the junctional T-tubules. In developing chicken muscle fibers the formation of peripheral couplings and the specific association of the SR with the Z-line precedes the formation of the T-tubules (Flucher *et al.*, 1993b), showing that these events are also independent of each other. However, the mature orientation of the T-tubules in the sarcomere takes place only after triads have been formed. In the present study we have investigated the sequence of the molecular specialization of junctional SR and T-tubules, the formation of T-tubule/SR junctions, and the onset and maturation of E-C coupling during normal development in vitro. The simultaneous and colocalized expression of DHPRs and RyRs, concomitant with the first appearance of junctions and E-C coupling function, suggests that the differentiation of the junctional domains of T-tubules and SR depends upon their interactions and leads directly to the formation of functional calcium release units.

MATERIALS AND METHODS

Cell Culture

The preparation of muscle cell cultures was performed as described (Daniels, 1990) except that the primary cell suspension was plated at 3.5×10^6 cells/100 mm diameter dish; Dispase (Boehringer Mannheim, Indianapolis, IN) was used at a concentration of 0.025%, and amphotericin B (2.5 μg/ml) (Fungizone, GIBCO/BRL, Gaithersburg, MD) was added to the culture medium. Briefly, cell suspensions were prepared by trypsin dissociation of 19–21-d-old fetal rat leg muscle and plated in 100 mm gelatin-coated tissue culture dishes. After 3 d, a suspension of cells enriched in myoblasts was obtained by mild digestion of the cultures with a neutral protease (Dispase). These cells were plated on glass coverslips coated with carbon and gelatin. To obtain extensive development of the contractile apparatus in the myotubes, the replated cell cultures were fed as follows. On the third day after replating, 5.4 μM FUdR and 13.2 μM uridine (final concentrations) were added to the culture medium already on the cells. This reduced the proliferation of nonmuscle cells without eliminating them. Three days later, and every 3–4 d thereafter, one-half of the medium was replaced with 90% Dulbecco's minimal essential medium (DMEM), 10% horse serum, 50 U/ml penicillin, 50 μg/ml streptomycin, and 2.5 mg/ml Fungizone.

Calcium Recordings

Recordings of intracellular free calcium concentrations were performed as described in Flucher *et al.* (1993a) with a dual-emission photometry system. Cultures plated on 25-mm round coverslips were rinsed once in serum-free DMEM without phenol red (GIBCO/BRL) and then incubated in the fluorescent calcium indicator fluo-3 AM (5 μM) and SNARF-1 AM (0.5 μM) plus 0.1% Pluronic F-127 (all from Molecular Probes, Eugene, OR) in the same medium for 30 min at room temperature. After another rinse the coverslips were transferred into the observation chamber (Leiden dish, Medical Systems, Greenvale, NY) and mounted on a Zeiss (Thornwood, NY) Axiovert inverted microscope. Electrical field stimulation was performed with a 1-ms pulse of 15–20 V passed across the 19 mm diameter well of the incubation chamber. Calcium measurements were carried out with epifluorescence using a narrow-band 488-nm filter for the simultaneous excitation of fluo-3 and SNARF-1. The illumination from a 100W xenon arc lamp was attenuated, and the illuminated area was restricted by closing the field diaphragm to just outside the field of observation. The fluorescence signals emitted during a calcium transient were strong enough to be seen with the naked eye through the eyepieces, which facilitated the screening of cultures. Fluorescent measurements from a field of 30×30 μm were performed with a Photon Technology International (PTI, South Brunswick, NJ) dual photometer system using a 590-nm dichroic mirror with a 530-nm barrier filter for fluo-3 and

a 610-nm barrier filter for SNARF-1 (Omega Optical, Brattleboro, VT). The two channels were routinely recorded at a sampling rate of 200 Hz, and the ratio of the two emission wavelengths was calculated using PTI Oscar software. For the analysis of the fast upstroke, 10 consecutive calcium transients were sampled at 1 kHz and averaged to reduce noise. Ratios of fluo-3/SNARF were independent of cell thickness and intensity of illumination, and calcium measurements with this combination of dyes were more sensitive than those obtained with the dual-emission calcium indicator Indo-1. Over the course of long experiments, the signal in the fluo-3 channel moved slowly upward (even without illumination) whereas the signal in the reference channel SNARF-1 remained stable. This indicates that some dye in the (acetyloxy)methylester form was continually hydrolyzed and thus increased the concentration of the active form of the calcium indicator in the cytoplasm. Normalizing the ratios (fluo-3/SNARF-1) to a common baseline value of one corrected for this drift and resulted in consistent records from a given measuring point over the period of 1 h or more. This normalization procedure also compensated for cell-to-cell differences in the relative efficiency of loading and hydrolysis of the two dyes.

Immunofluorescence Labeling

Cultures were fixed in 100% methanol at −20°C for 10 min, rehydrated by plunging into phosphate-buffered saline (PBS) at room temperature, and then rinsed in several changes of PBS. Subsequently, the cultures were incubated with 10% normal goat serum in PBS containing 0.2% bovine serum albumin (BSA) (PBS/BSA) for 30 min or longer and then incubated in primary antibodies for ≥2 h at room temperature or overnight at 4°C. After washing in five changes of PBS/BSA, the cultures were incubated in fluorochrome-conjugated secondary antibodies for 1 h at room temperature and washed again. Finally, they were mounted in 90% glycerol, 0.1 M tris(hydroxymethyl)aminomethane pH 8.0 with 5 mg/ml p-phenylene diamine to retard photobleaching.

The semiquantitative analysis of labeling patterns was performed by screening double-labeled coverslips with a 40× objective on a Zeiss Axioskop fluorescence microscope and scoring all segments of myotubes visible at one time in the field. If clustered distribution of both antigens was observed, regardless of the degree of maturation (random or cross striated organization), the myotube was rated as "clustered."

Antibodies

For the localization of the DHPR, the mouse monoclonal antibody 1A (specific for the skeletal muscle α_1 subunit) was used at a concentration of 0.1 μM IgG (Morton and Froehner, 1987). A sequence-specific antibody against the ryanodine receptor (anti-RyR#5) was used at a dilution of 1:5000. Anti-RyR#5 was prepared against a synthetic peptide corresponding to a RyR amino acid sequence specific for the skeletal muscle isoform from rabbit (amino acids 1333–1353) (Flucher *et al.*, 1993a). Various combinations of the following secondary antibodies were used: rhodamine- or fluorescein-conjugated goat anti-mouse IgG (BCA/Cappel Products, Organon Technika, Malvern, PA) at dilutions of 1:500 and 1:300, respectively; lissamin-rhodamine-conjugated goat anti-mouse and goat anti-rabbit IgG both at 1:200; Cy-3-conjugated donkey anti-mouse (Jackson Immuno-Research Laboratories, West Grove, PA) at 1:4000; fluorescein-conjugated goat anti-rabbit IgG (Miles Scientific, Naperville, IL) at 1:400.

Confocal Microscopy and Cluster Analysis

Myotubes labeled with the antibodies against the DHPR and RyR were viewed on a BioRad MRC-600 (Richmond, CA) confocal microscope equipped with the filter sets for simultaneous double immunofluorescence. Zeiss 63× 1.4 NA and 100× 1.3 NA lenses were used. The adjustable pinhole was set to 0.4 where the thickness of the optical section was determined to be ≈0.3 μm. Images were recorded at 1-μm intervals starting at the surface of the myotube. To avoid bias for one of the two antibodies because of differences in labeling intensity or the sensitivity of the respective channel, the fluorochrome-conjugated secondary antibodies were switched in several experiments.

For the analysis of density and size of clusters, images from all developmental stages were imported into the National Institutes of Health (NIH) Image program (W. Rasband, National Institute of Mental Health/NIH, available from National Information Technology Services, Alexandria, VA). The area of the cytoplasm (excluding nuclei) was measured. The grayscale images were converted to black and white, and the thresholds were adjusted by eye for maximal correspondence of the images in both channels. Clusters were counted and their area was measured. Results from two independent measurements of the same pair of images were highly consistent. Data were analyzed according to culture age and location of the optical section (periphery or center). However, individual, densely packed small clusters from myotubes 10 d after replating could not be adequately resolved by this method.

Electron Microscopy and Junction Analysis

Fixation, embedding, and sectioning of the muscle cell cultures were performed as described previously (Olek *et al.*, 1986), except that the initial 15 min of fixation was done without tannic acid. Briefly, cells were fixed in cacodylate-buffered glutaraldehyde for 15 min at room temperature then in the same fixative with the addition of 0.15% tannic acid for 15 min at room temperature and 1 h at 4°C. Cultures were postfixed with osmium tetroxide, then en bloc stained with uranyl acetate, and embedded in Epon after dehydration. Typical regions of cultures fixed at 3, 5, 7, and 10 d after myoblast replating were trimmed and sectioned either perpendicular to the long axis of the myotubes or perpendicular to the culture substrate but parallel to the long axis of the myotubes. Thin sections (~80 nm) were stained with uranyl acetate and lead citrate and viewed with a JEOL 1200 EXII electron microscope (Peabody, MA).

To quantitate the abundance of junctions between SR and T-tubules, the sections were scanned at 5000× magnification (such that junctions could not be seen while scanning) to systematically sample the myotube profiles. For each time point, 3–13 micrographs of each of 7–10 myotubes were taken at the same magnification. The micrographs were printed at a final magnification of 13 500× and examined under a magnifying illuminator. All junctions between SR and T-tubules were identified and classified as to their configuration (see RESULTS). The cytoplasmic area in each micrograph was measured with a digital tablet and the number of junctions per 1000 μm^2 of cytoplasm was calculated. Junctions between SR and T-tubules were defined by a close apposition between SR cisternae (having a relatively electron-dense lumen) and the relatively lucent T-tubules and the presence of dense material within the junction. This characteristic structure was easily recognized even if the junctional feet were not resolved because of the plane of the section. In the micrographs of 10-d-old myotubes, cytoplasmic areas lacking myofibrils (usually in the central cytoplasm in between nuclei), and adjacent areas of similar size that were densely packed with myofibrils, were outlined and assayed in the same manner for the abundance and configuration of junctions. The measure of the abundance of junctions used here (area density) should be taken as an operational measure of the relative density of junctions. Because both the size and orientation of the junctions changes with development (see RESULTS), it would be difficult to interpret these measurements in terms of the number of junctions per unit of cytoplasmic volume.

RESULTS

Action Potential-induced Calcium Transients

The onset of E-C coupling in primary cultures of rat skeletal muscle was observed on the second day after replating, which is ~1 d after myoblast fusion. Cultures

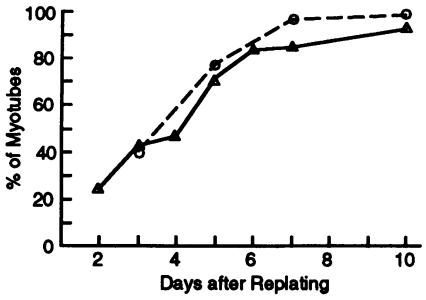

Figure 1. Development of E-C coupling compared to formation of DHPR/RyR immunoreactive clusters in rat myotubes. Cultures of different ages were incubated with fluo-3 and systematically screened for myotubes generating calcium transients in response to electrical stimulation (——). Parallel cultures were immunolabeled and screened for colocalized DHPR and RyR clusters (- - -). The increase in the percentage of active myotubes is closely accompanied by an increase in myotubes expressing DHPR/RyR clusters. Total numbers of myotubes counted for each data point ranges from 133 to 494.

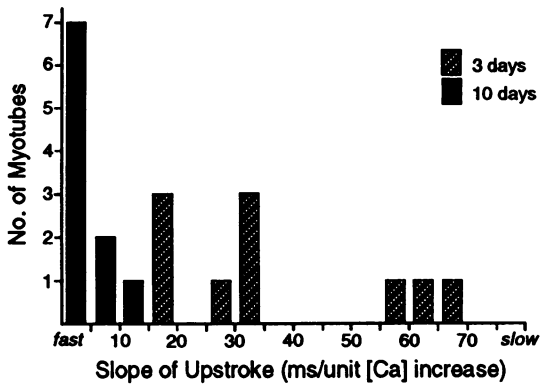

Figure 3. Calcium release rates increase during myotube development. Action potential-induced calcium transients were recorded with 1-ms time resolution in myotubes of 3- and 10-d-old cultures. The slope of the linear portion of the upstroke—a function of the release rate—was determined from the average of 10 consecutively stimulated transients in each of 10 myotubes per stage. The frequency distribution shows that the upstrokes of transients in young myotubes are relatively slow and scattered over a wide range of speeds whereas mature myotubes are consistently fast.

simultaneously loaded with the fluorescent calcium indicator fluo-3 and SNARF-1 (used as reference dye in dual emission calcium measurements; see MATERIALS AND METHODS) were excited by field stimulation. Myotubes competent for E-C coupling responded to such a stimulus with a transient increase of cytoplasmic free calcium (see below), which was often accompanied by a visible twitch. Myotubes responded in an all-or-none fashion to gradually increased voltages of the pulse; calcium transients could be blocked by tetrodotoxin and could be modulated by 2 mM caffeine. Furthermore, they were virtually indistinguishable from calcium transients that occur during spontaneous contractile activity (Flucher and Andrews, 1993). Thus, these transients represent action potential-induced release of calcium from intracellular stores, that is, E-C coupling. On the second day after replating, one-quarter of all myotubes were E-C competent. The proportion of active myotubes increased steadily to more than 90% by day 10 after replating (Figure 1).

The transient increase of cytoplasmic free calcium in response to electrical stimulation is characterized by a rapid rising phase and an immediate, exponential decay at a slower rate. Figure 2 shows representative examples of calcium transients stimulated by individual pulses and by a 2.5-s stimulus train at 20 Hz. The records are sorted in descending order of the time constants for the exponential decay of the transients (a, slowest; e, fastest). Repeated action potential-induced calcium tran-

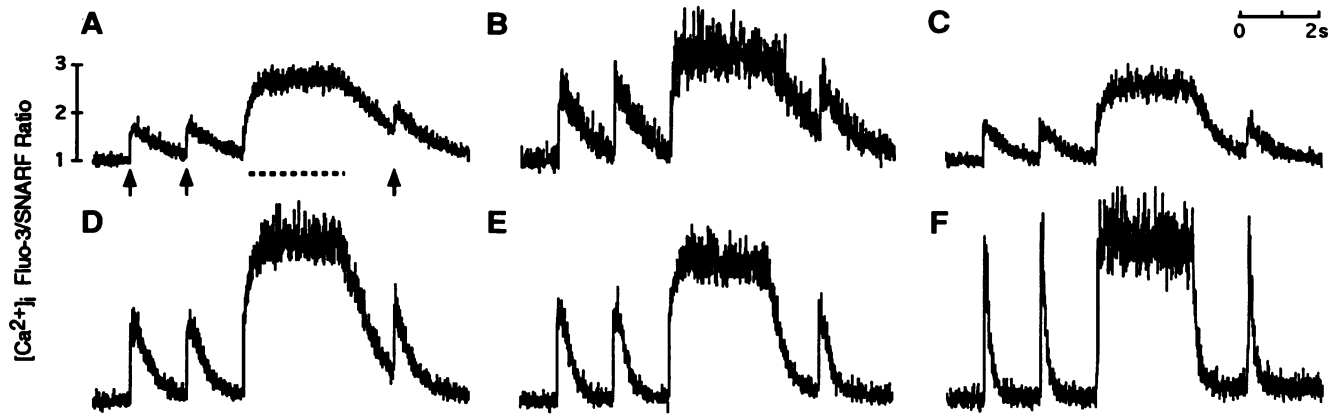

Figure 2. Action potential-induced calcium transients in young myotubes. Myotubes loaded with fluo-3 and SNARF-1 were electrically stimulated (single pulses, arrows; stimulus train, 20 Hz, - - -), and cytoplasmic calcium concentrations were recorded with dual-emission microfluorometry (see MATERIALS AND METHODS). Repeated stimulation of individual myotubes resulted in consistent calcium transients. Different myotubes in 4-d-old cultures (A–E) varied considerably in peak amplitudes and decay times of calcium transients. In 10-d-old myotubes (F) calcium transients showed mature characteristics. x-axis, arbitrary ratio units; y-axis, 10-s traces.

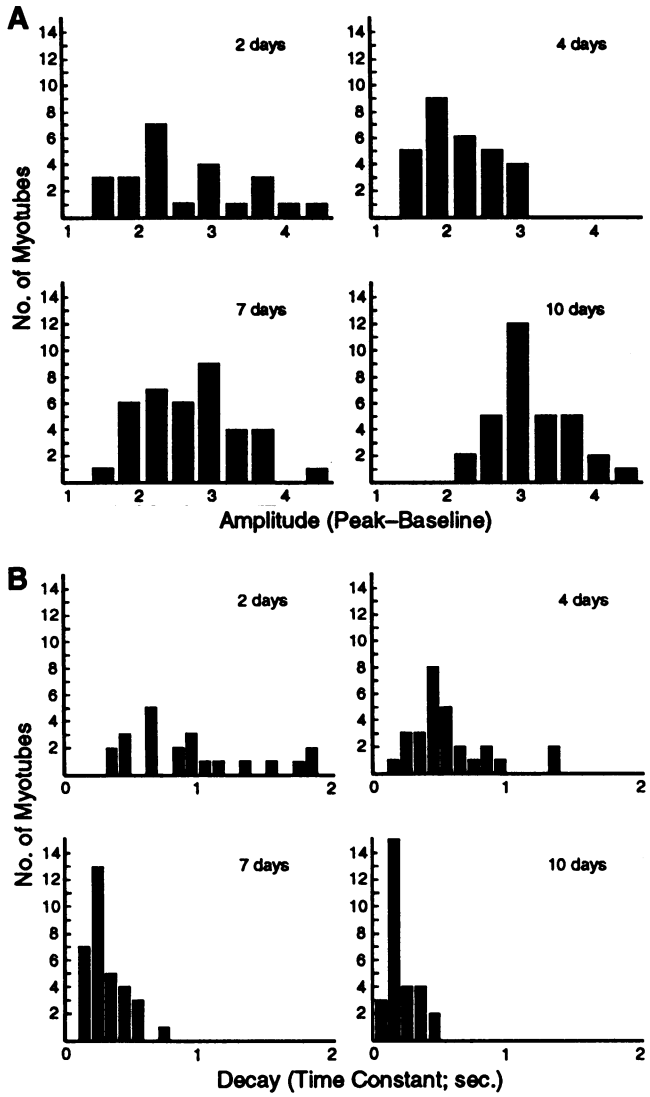

Figure 4. Developmental change in amplitude and decay of action potential-induced calcium transients. (A) The difference between resting and peak levels of calcium was measured in electrically stimulated transients in 2-, 4-, 7-, and 10-d-old cultures. The frequency distribution of peak amplitudes of myotubes shows little change during the first week but a slight increase by day 10. (B) Rates of the exponential decay—a function of calcium uptake into the SR—increase significantly over the entire observation period. With time in culture, the variability between myotubes of the same age decreases for both parameters.

sients recorded from a given myotube were highly constant in shape (compare the 3 individual transients of each record). Different myotubes from one culture, however, varied significantly in size and shape of the transients. During a stimulus train the calcium concentration continues to rise at a slow rate after the initial rapid upstroke, asymptotically approaching a plateau value that is usually higher than that of an individual transient. This indicates that the calcium store of the myotubes is not exhausted during an individual transient and therefore does not represent the limiting factor for the amplitude of a transient. Upon termination of the stimulus train, calcium levels decay at about the same rate as in individual transients. The difference between amplitudes of individual action potential-induced transients and those during tetanic stimulation is usually greater in myotubes with low peak amplitudes and/or slow decay rates of single transients. Thus, maturation of the calcium stores seems to precede that of the release apparatus. Most myotubes of 10-d-old cultures had calcium transients with high amplitudes and fast decay rates (Figure 2F). These mature myotubes showed little difference in peak amplitudes between individual and tetanic calcium transients.

Three parameters of the transient increase of cytoplasmic free calcium—the amplitude and the rates of upstroke and decay—were individually analyzed and compared in cultures of different ages. At a single developmental stage, considerable variability in each one of these parameters was apparent. However, variability between myotubes was generally greater in younger cultures than in older ones. This tendency probably reflects the heterogeneous population of myotubes in young cultures. Because myoblast fusion continues over a period of several days, myotubes of different devel-

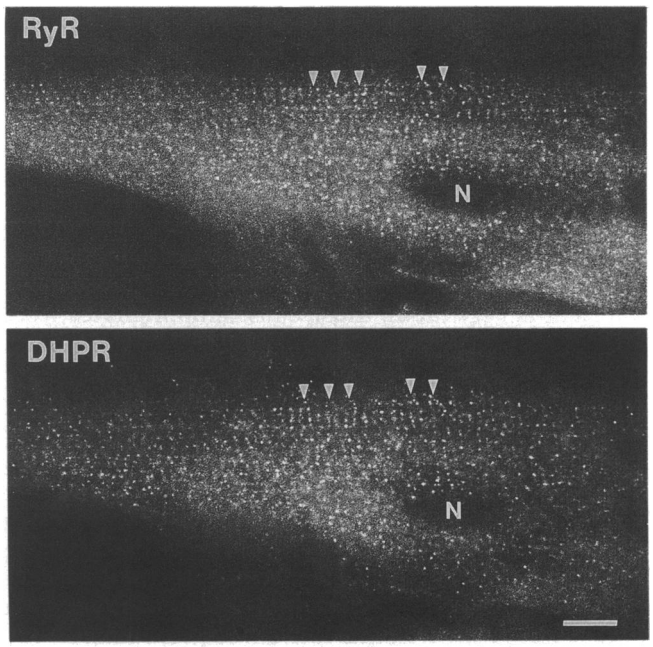

Figure 5. Distribution of RyR and DHPR in a mature skeletal myotube. Rat myotubes 11 d after replating were double-immunolabeled with antibodies against the RyR and DHPR and fluorochrome-conjugated secondary antibodies. RyR and DHPR are colocalized in discrete clusters that form double rows transversely to the long axis of the myotube. The center-to-center distance between two adjacent double rows of clusters (examples indicated by arrowheads) corresponds to a sarcomere's length (≈2.5 μm). N, nuclei; bar, 10 μm.

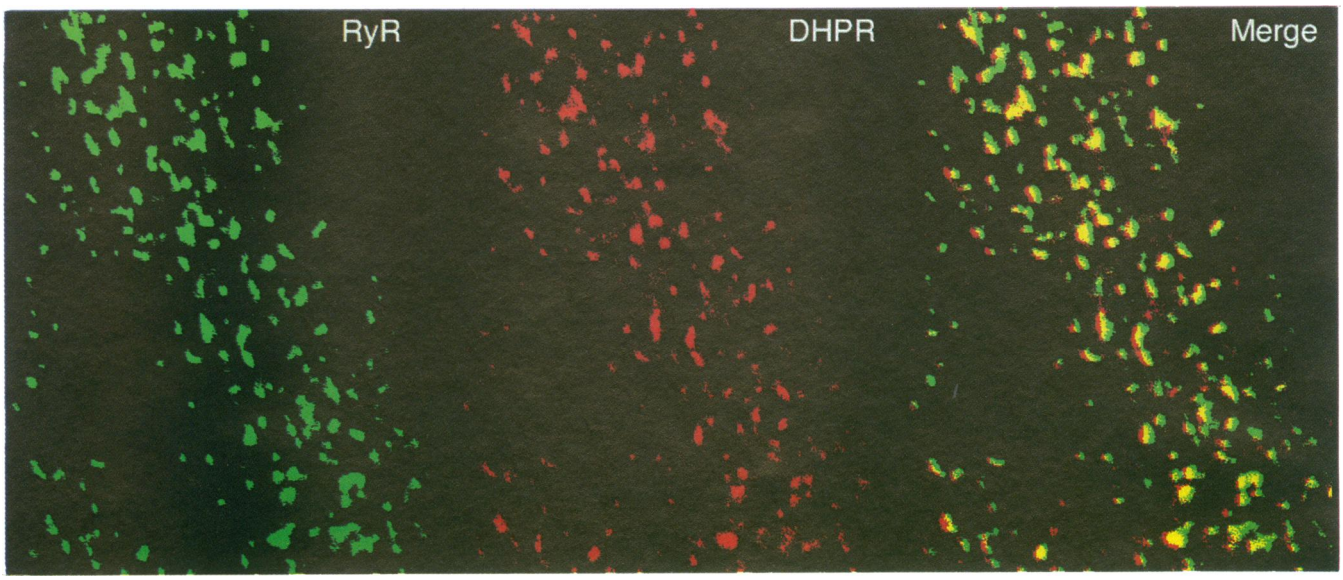

Figure 6. Colocalization of RyR and DHPR in clusters of young myotubes. Optical sections (≈0.3 μm thickness) of a 5-d-old myotube labeled for RyR and DHPR were thresholded and merged with a horizontal offset of 4 pixels (≈0.5 mm in the print) (Merge). The resulting red-yellow-green pattern in large clusters and the red-green apposition in small clusters indicates colocalization of RyR and DHPR, while still allowing one to see the shape of the individual clusters.

opmental stages are simultaneously present in a culture, giving rise to differences in all aspects of calcium regulation. Once the formation of new myotubes is completed the action potential-induced transients become more uniform. At a single stage calcium transients tended toward higher amplitudes in myotubes with faster decay rates (Figure 2, A, D, and E). However, a minority of myotubes did not show this correlation (e.g., Figure 2, B and C). Thus, the maturation of the amplitude and rate of decay may proceed in parallel but are not necessarily linked to one another.

The upstroke of an action potential-induced calcium transient is very rapid; thus, 1-ms sampling rates were required to record this part of the transient with adequate time resolution. To reduce instrumental noise, 10 consecutive traces from one measuring point were recorded and averaged. Such averaged recordings were obtained from 10 randomly chosen myotubes of 3- and 10-d-old cultures. Fits of the linear portion of the upstrokes yielded time constants of 15 ms/fluorescent ratio unit or higher in myotubes at 3 d, but at 10 d the time constants averaged only 4 ms/ratio unit (Figure 3). The upstroke of a calcium transient corresponds to calcium release from the SR minus calcium sequestration by cytoplasmic buffers and the SR. Changes in the slope of the early, linear portion of the upstroke are likely to represent changes in the rate of calcium release. The frequency distribution of the analyzed myotubes (Figure 3) also shows that the variability of release rates between myotubes of 3-d-old cultures was very great, whereas at day 10 the rates were nearly constant. Even in the younger cultures the slopes of the upstroke were generally higher in calcium transients that reached greater peak amplitudes. However, transients were also recorded that had fast rise times and small amplitudes or visa versa. Thus, peak levels of cytoplasmic free calcium during a transient are not a simple function of the release rates. Likewise, rise times and rates of exponential decay are not well correlated. This suggests an independent development of release and reuptake activity, which ultimately reside in junctional and longitudinal SR, respectively.

Developmental changes of amplitudes and of the decay of action potential-induced calcium transients were studied in myotubes from days 2, 4, 7, and 10 after replating (examples shown in Figure 2). Analysis of recordings from 30 to 40 myotubes of each stage showed developmental changes in the mean values and the variability of both parameters (Figure 4): first, a maturation of transients toward greater amplitudes and faster decay rates and second a decrease in variability. In day 2 myotubes, the peak amplitudes of the transients—defined as maximal increase of the fluo-3/SNARF-1 ratio above resting calcium levels—were scattered over the range of 1 to 4.5 with more than one-half of the myotubes showing ratios below 2.5 (Figure 4A). On day 10 the amplitudes were distributed within the range of 2 to 4.5 with a peak at 3. The time constants for exponential decay of the transients ranged from 0.3 to 1.9 s in 2-d-old myotubes but were consolidated at day 10 into a range below 0.5 s with a peak at 0.15 s (Figure 4B). Thus, amplitude and rate of decay of the transients

Table 1. Density of DHPR/RyR clusters

Days in culture	DHPR clusters/1000 μm^2	RyR clusters/1000 μm^2
3	104 (±7.0)	130 (±9.5)
5	154 (±12.7)	144 (±12.5)
7	190 (±10.9)	189 (±8.2)

The density of clusters of DHPR and RyR were analyzed individually in confocal images of ≈0.3 μm optical section thickness (see MATERIALS AND METHODS). Values given are the mean ± SE (n, 33–50 images per stage).

(as well as the rate of the upstroke) are all subject to continued change after the basic function of E-C coupling is established. Furthermore, the cultures became increasingly homogeneous with respect to all three parameters so that functional properties of 10-d-old cultures were similar to those of mature muscle fibers in vivo (Eusebi *et al.*, 1980).

Codistribution of DHPR and RyR

In parallel with the increased number of active myotubes the number of myotubes expressing the α_1 subunit of the DHPR and the RyR increased steadily (Figure 1). The close temporal correlation of the development of contractile activity and the appearance of DHPR/RyR-immunoreactive clusters suggests that the onset of E-C coupling in skeletal muscle is tightly linked to the expression and colocalization of the DHPR and RyR. To correlate the developmental changes of E-C coupling properties with the abundance and distribution of DHPR/RyR clusters, myotubes from different developmental stages were immunolabeled and analyzed on a laser scanning confocal microscope. The two key proteins in E-C coupling—the presumptive voltage sensor and the SR calcium release channel—were colocalized in clusters. In mature, cross-striated myotubes DHPR/RyR clusters were aligned in double rows, which were oriented perpendicular to the long axes of the myotube (Figure 5). This disposition corresponds to the staining pattern of DHPR and RyR in vivo and to the position of triads at the A-I border in the sarcomere of mammalian skeletal muscle. At earlier developmental stages clusters of DHPR and RyR were randomly distributed in the cytoplasm and heterogeneous in size. Nevertheless, both proteins were almost always colocalized (Figure 6), indicating a position at contact sites between T-tubules and the SR.

The distribution patterns of DHPR/RyR-immunoreactive clusters changed over time in a characteristic manner (Figure 7). In young cultures (3 and 5 d) most myotubes expressing the ion channels showed low densities of large DHPR/RyR clusters of variable shapes throughout the cytoplasm. The density of clusters increased steadily over the observation period. In parallel, their size decreased and their shape and distribution became more uniform. Quantitative analysis of myotubes labeled with DHPR and with RyR showed a high degree of correspondence in the numbers of clusters per myotube segment for each antibody (Table 1), suggesting that both channels become incorporated into clusters simultaneously. Small deviations between the two antibodies in single myotube segments occurred

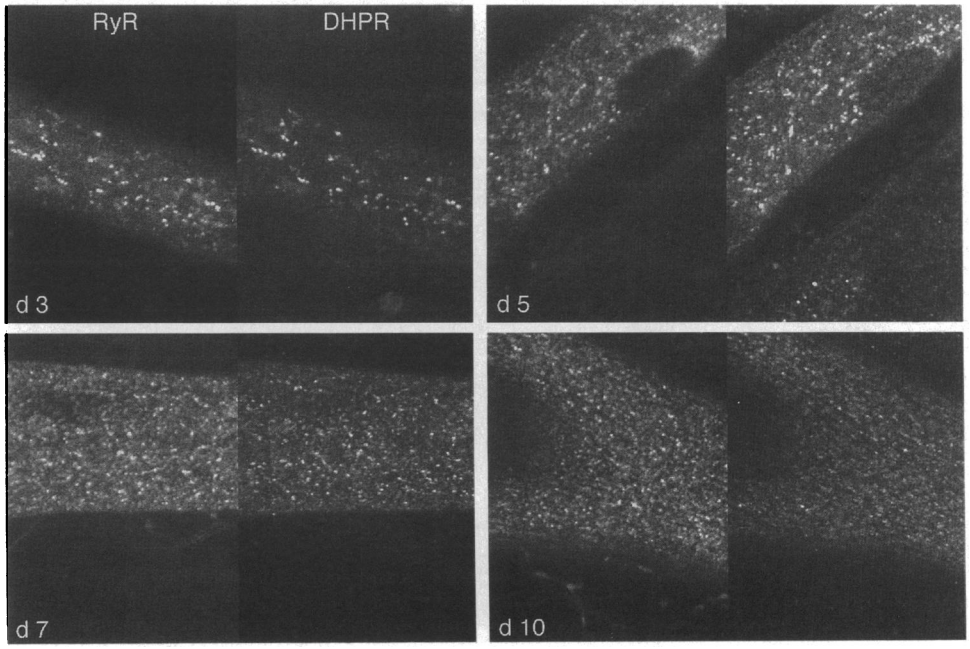

Figure 7. DHPR and RyR are expressed simultaneously and colocalized in developing myotubes. Rat myotubes, 3, 5, 7, and 10 d after replating, were double immunolabeled with antibodies against the RyR (left) and DHPR (right of each pair) and 0.3 μm thick optical sections were recorded. Both proteins first appear colocalized in clusters that are randomly distributed throughout the cytoplasm. Over time the density of the clusters increases and they become more evenly distributed.

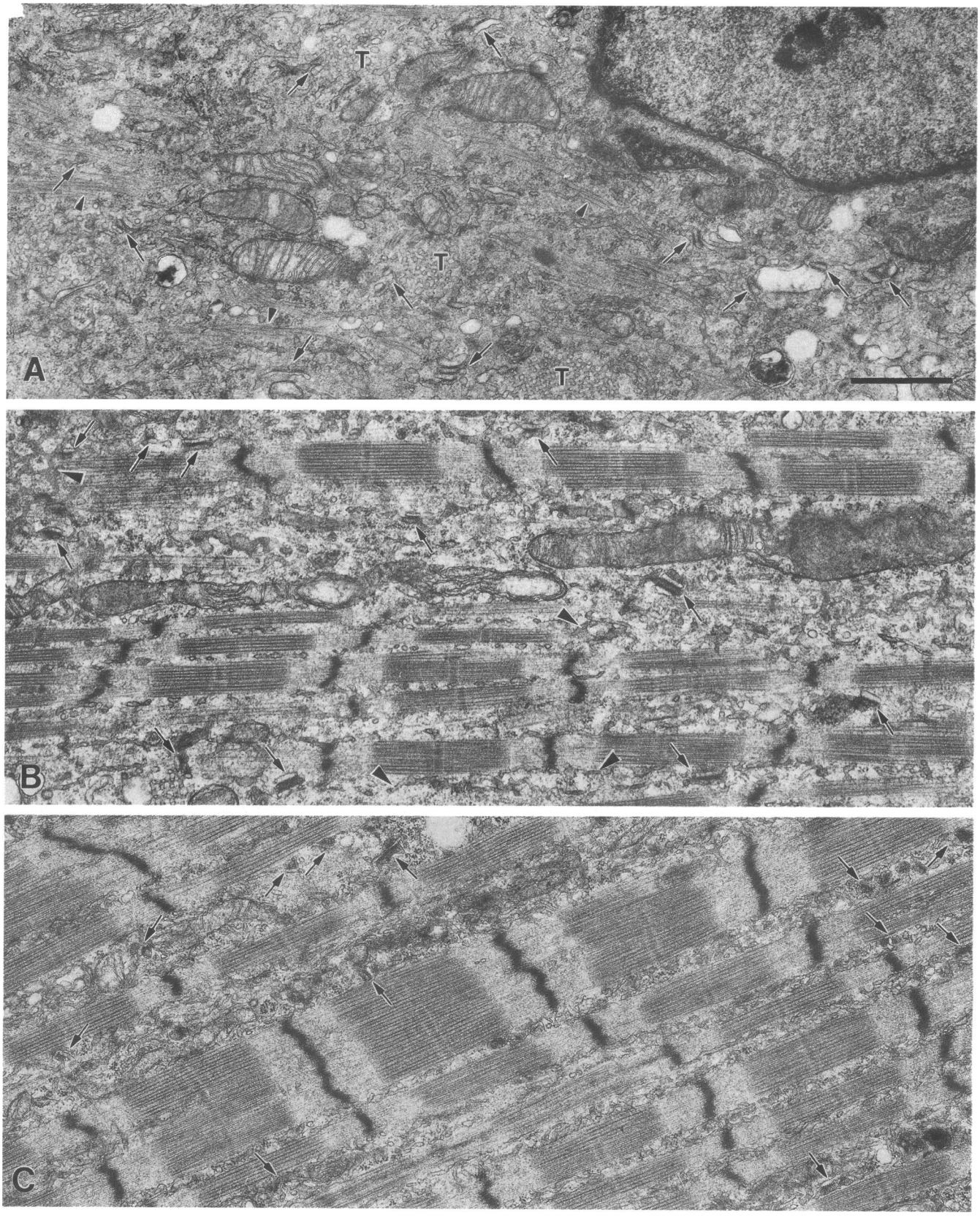
T
T
T
A
B
C

but were random with respect to the antibody. This discrepancy may arise from different labeling efficiencies of the two antibodies or, less likely, may indicate the existence of a small number of DHPR and RyR clusters without the respective counterpart. Table 1 also shows a steady increase in the mean density of clusters in ~0.3 μm thick optical sections for myotubes 3, 5, and 7 d after replating. The dramatic increase in density and decrease in size of clusters that is apparent on inspection at day 10, as seen in confocal images (see Figure 7) and in the electron micrographs (see below), was not detected because of the limited resolution of the automated analysis.

Formation of T-Tubule/SR Junctions

At the same time as myotubes expressed the first DHPR/RyR clusters and when they became responsive to stimulation, junctions between T-tubules and SR could be observed in electron micrographs. At 3 d these junctions were randomly distributed throughout the cytoplasm, and their abundance was roughly comparable to that of DHPR/RyR clusters, taking into account the difference in section thickness. They were commonly found in the perinuclear region, which tends to be devoid of myofibrils at this stage (Figure 8). Early junctions formed in a variety of conformations and sizes (Figure 9): diads (1 T-tubule, 1 SR cisterna), standard triads (1 T-tubule between 2 SR cisternae), inverted triads (1 SR cisterna between 2 T-tubules), and multiple junctions (2 or more of each compartment) (Schiaffino *et al.*, 1977). Junctional T-tubules were often continuous with caveolae-like elaborations of the T-system (Figures 8A, and 9, A and D) (Ishikawa, 1968; Franzini-Armstrong, 1991), and junctional SR could be continuous with adjacent segments of rough ER (Figure 9D). Despite the irregular configurations, these junctions showed the membrane specializations of mature triads. The lumen of the SR contained electron dense material, and the gap was spanned by regularly spaced feet. At later developmental stages the myotubes filled with myofibrils, confining membrane compartments and their junctions into the narrow spaces between the myofibrils and to domains next to nuclei that lacked myofibrils. The overall density of junctions and the proportion of standard triads increased sharply between 7 and 10 d (Table 2). In addition, the size of the junctional profiles decreased (compare Figure 9A to 8C). Because of this decrease in size, the observed increase in the number of junctions per unit area probably is an underestimate of the increase in junctions per cytoplasmic volume (see MATERIALS AND METHODS). SR was more abundant at 7 and 10 d than in younger cultures, and it tended to accumulate at the I-band of the myofibrils (Figures 8B and 9B), which is consistent with an earlier observation of cross-striated organization of α-actinin and the SR Ca^{2+}-ATPase in mouse myotubes (Flucher *et al.*, 1992). Although T-tubules were still predominantly longitudinally oriented, the triads began to associate with the myofibrils at the A-I junction, which is their location in mature rat muscle. Only in a final step did the triads become reorganized into the transverse orientation (Figure 9E).

Standard triads were closely associated with the myofibrils, frequently near the A-I junction. In contrast, nonstandard junctions were less often associated with myofibrils. In the myofibril-rich domain of 10-d-old myotubes, the total density of junctions was three times higher than in the myofibril-poor domain. This difference could primarily be accounted for by an eightfold higher density of standard triads in the myofibril-rich region, whereas nonstandard configurations did not differ significantly between the two domains (Table 3). In immunofluorescence this condition manifested itself in the decrease of cluster size, a higher uniformity of size and distribution, and ultimately in the cross-striated arrangement of DHPR/RyR clusters. The latter represents the transverse organization of triads. The transition from large, randomly oriented clusters to uniformly distributed small clusters could be seen in individual myotubes progressing from the periphery toward the center of the myotubes (Figure 10). This trend corresponds to the course of myofibrillogenesis, which also progresses from the periphery toward the center. Thus, the mechanisms that determine the configuration of standard triads appear to be closely linked to the maturation of the myofibrils.

A minor population of DHPR/RyR-positive myotubes at day 3 and 5 showed either no clusters in the cytoplasm at all, or myotube segments with few or no cytoplasmic clusters. Instead these myotubes expressed DHPR/RyR clusters at the cell surface (Figure 11, A and B). Such peripheral clusters were commonly found in rows running in parallel with the long axis of the myotube. This labeling pattern was only rarely observed

Figure 8. Developing myotubes contain T-tubule/SR junctions whose sizes and distributions resemble those of DHPR/RyR clusters. Location of junctions (examples of which are shown at higher magnification in Figure 9) are indicated by arrows. In myotubes fixed 3 d after replating (A), large junctional profiles are found throughout the cytoplasm, commonly in regions close to nuclei. Junctional T-tubule profiles are usually dilated. The junctions show no obvious association with the sparse developing myofibrils (small arrowheads). The junction-rich regions contain an abundant network of T-tubules, including caveolae-like arrays (T). At 7 d (B) profiles of junctions remain large and are often associated with the extensively developed myofibrils. There is an abundance of SR cisternae in between the myofibrils (examples indicated by large arrowheads). At 10 d (C) the sarcomeres of the myofibrils are partially aligned. The profiles of junctions are smaller than at earlier stages and are predominantly associated with the myofibrils. The spaces between the myofibrils are packed with SR and mitochondria. Bar, 1 μm.

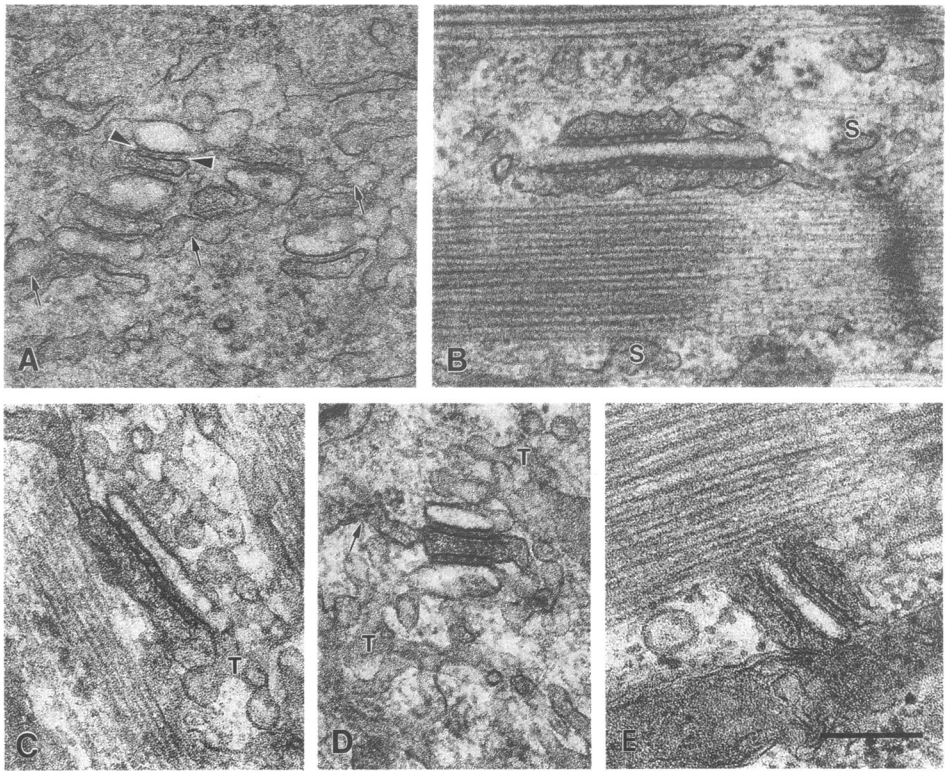

Figure 9. Configuration and orientation of T-tubule/SR junctions in developing myotubes is variable. (A) A large "multiple" junction in a myotube fixed 3 d after replating contains five T-tubule profiles (a long profile associated with 4 SR cisternae is indicated with arrows) and seven SR cisternae, which can be identified by their electron-dense content. Arrowheads indicate a junctional region with clearly defined feet. (B) A longitudinally oriented "standard" triad associated with a myofibril in a 7-d myotube. The T-tubule profile is narrow and feet are clearly visible. Examples of nonjunctional SR are indicated (S). (C) A "diad" in a 5-d myotube. Note the caveolae-like organization of the nonjunctional T-tubule (T). (D) An "inverted triad" in a 7-d myotube. The single SR profile is connected to the rough endoplasmic reticulum (arrow). The T-tubule profiles of the junction are connected to an elaborate T-tubule network (T). (E) A transversely oriented "standard" triad on a 10-d myotube. The triad is located close to the A-I interface of the myofibril. Bar, 0.2 μm.

in older cultures. Electron micrographs of young cultures revealed myotubes with frequent peripheral couplings—junctions between the SR and the plasma membrane (Figure 11, C and D). The peripheral couplings had regularly spaced feet and most probably correspond to the peripheral clusters labeled with antibodies against the skeletal isoforms of DHPR and RyR.

DISCUSSION

At least three separate events contribute to the formation of the skeletal muscle triad: 1) the specialization of the junctional domains of T-tubules and SR, 2) the association of the two membrane compartments to form a functional junction, and 3) the determination of the triad structure and its orientation in the sarcomere. The molecular differentiation of the junctional membranes could occur independently in T-tubules and SR, before the formation of the junction, or it could occur simultaneously in an interdependent process (Flucher, 1992). Another possibility would be the sequential organization of the complex, starting with the differentiation of one compartment, which would subsequently contact the other compartment and thus induce its differentiation. Independent differentiation of one or both junctional domains should result in separate and successive clus-

Table 2. Density of T-tubule/SR junctions

	T-tubule/SR junctions/1000 μm^2				
Days in culture	Total	Diads	Inverted triads	Standard triads	Multiple junctions
3	27 (±8.3)	5.5 (±1.8)	2.4 (±1.1)	2.3 (±0.7)	2.0 (±0.8)
5	19 (±4.2)	6.7 (±1.8)	5.0 (±1.4)	4.5 (±1.4)	1.8 (±0.8)
7	42 (±6.3)	7.8 (±1.9)	4.5 (±1.0)	7.9 (±1.4)	6.4 (±1.2)
10	122 (±8.8)	39.3 (±4.6)	7.6 (±1.1)	66.8 (±5.6)	9.3 (±1.8)

T-tubule/SR junctions were counted in electron micrographs of 80 nm-thick sections like those shown in Figure 8. Values given are the mean ± SE (n, 7–10 myotubes per stage, 3–13 micrographs each); total junctions represent a larger data set than individual types, because some junctions at each stage were unidentifiable.

tering of the DHPR and/or the RyR. However, this does not appear to be the case. Our observation that both membrane proteins are expressed simultaneously in colocalized clusters, together with the failure to detect significant independent clustering, suggests that the differentiation of both junctional membranes occurs after their initial contact with one another. Thus, it is possible that contact between unspecialized T-tubules and SR may indeed induce the differentiation of their junctional domains. The abundance, size, and distribution of the earliest junctions observed in electron micrographs are consistent with those parameters of DHPR/RyR clusters, indicating that DHPR/RyR clusters indeed correspond to T-tubule/SR junctions. Furthermore, the junctional membrane domains of T-tubules and SR already show the structural characteristics of a differentiated junction, and myotubes expressing DHPR/RyR clusters are capable of E-C coupling. Thus, there seems to be little delay between formation of the junction, differentiation of its membranes, and the development of its function. This is consistent with the model in which contact between T-tubules and SR initiates triad formation.

The mechanism that establishes the contact between T-tubules and SR could be either directed or random. The earliest junctions are randomly distributed and the type and size of these junctions generally reflects the relative abundance of the two membrane systems in the vicinity (Schiaffino *et al.*, 1977). This suggests that junction formation occurs by chance and not by a directed combination of one T-tubule with two SR cisternae. Simultaneous and colocalized expression of DHPR's and RyRs have also been observed in developing rabbit muscle in vivo (Yuan *et al.*, 1991). The first DHPR/RyR clusters appeared to be isolated from the T-tubule marker T28. Thus, it has been suggested that junctional T-tubule membranes are packaged and transported separately from those of nonjunctional T-tubules and that DHPR-containing vesicles associate with RyR-containing membranes to form triad precursors before their insertion into the T-system. However, using different T-tubule markers in cultured rat and mouse myotubes, we observed that T-tubule formation precedes the expression of DHPR/RyR clusters and that

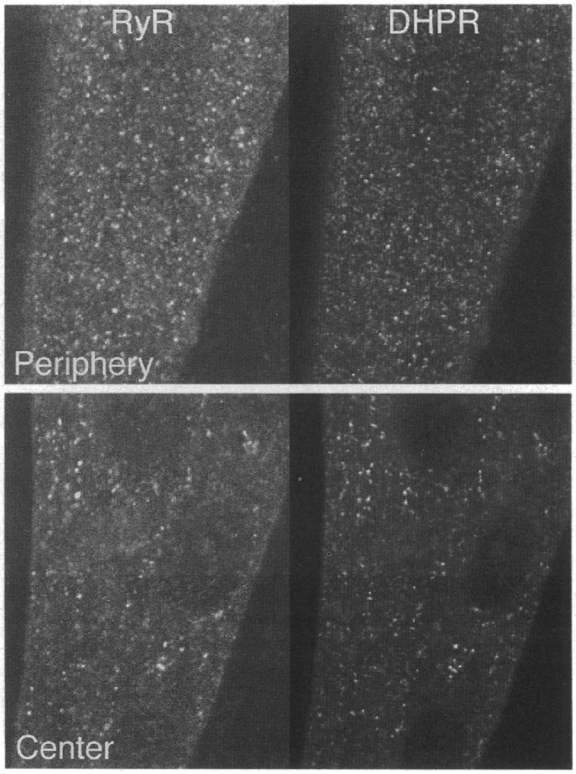

Figure 10. Density of DHPR/RyR clusters is higher in the periphery of the myotubes than in their center. Optical sections from the periphery and the center of a 7-d-old rat myotube that was immunolabeled for RyR (left) and DHPR (right). The region of high density of DHPR/RyR clusters in the periphery of the myotube corresponds to the myofibril-rich domains as seen by electron microscopy. Dark shapes in center section represent profiles of nuclei.

DHPR clusters are colocalized with T-tubules at all stages of development (Flucher *et al.*, 1991a, b, 1993b). Furthermore, the close correlation between the first appearance of DHPR/RyR clusters and the development of action potential-induced Ca^{2+} release (present study) indicates that, at least in culture, the clusters are functional junctions involving T-tubules continuous with the plasma membrane. The possible involvement of molecular interactions between the DHPR and RyR in the

Table 3. Distribution of T-tubule/SR junctions with respect to myofibrils

	T-tubule/SR junctions/1000 μm^2 at day 10				
Cytoplasmic domain	Total	Diads	Inverted triads	Standard triads	Multiple junctions
Myofibril-rich	165.5 (±13.0)	54.2 (±9.4)	5.8 (±5.0)	88.2 (±10.1)	17.5 (±14.4)
Myofibril-poor	52.2 (±11.1)	30.8 (±8.0)	8.6 (±6.0)	10.1 (±4.4)	2.7 (±2.7)

T-tubule/SR junctions were counted in cytoplasmic regions lacking myofibrils and in adjacent, myofibril-rich regions of similar size. Values given are the mean ± SE (n, 8 myotubes, 1–4 micrographs each).

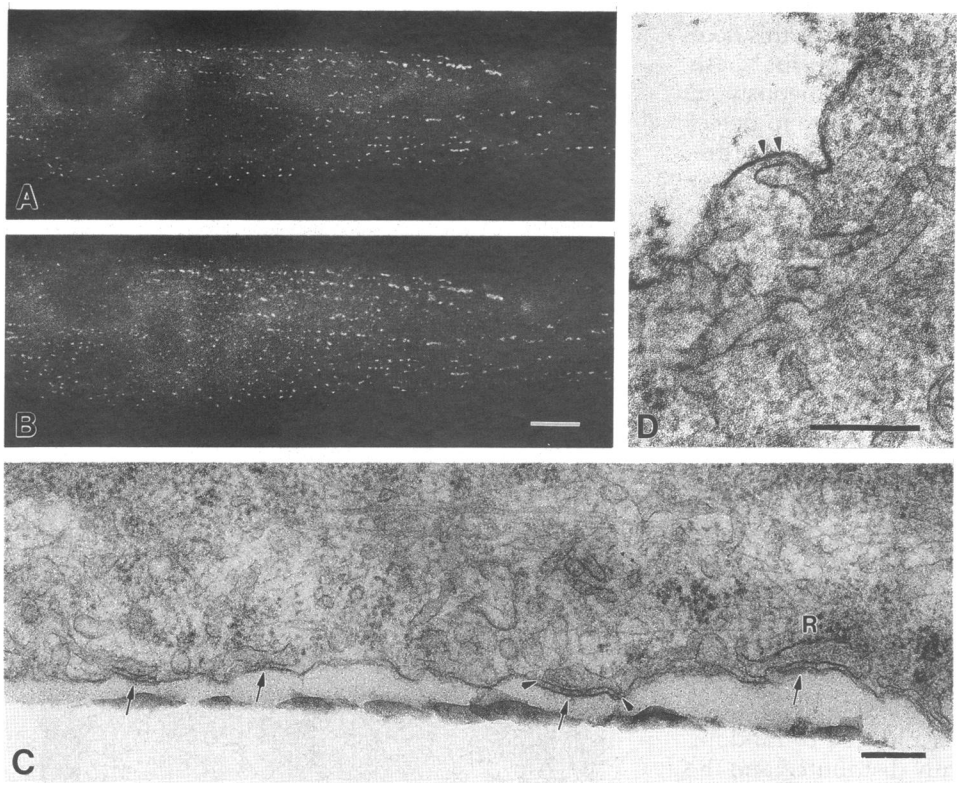

Figure 11. DHPR/RyR clusters corresponding to peripheral couplings are found at the surfaces of some developing myotubes. (A and B) Immunoreactivity for the RyR (A) and DHPR (B) is colocalized in clusters arranged in longitudinal rows on the upper surface of a 5-d myotube. (C) Junctions (peripheral couplings) between the SR and the plasma membrane (arrows) at the lower surface of a 5-d myotube that was sectioned parallel to the long axis of the myotube. Feet are most clearly seen in the junction indicated with arrowheads. The cisterna forming one of the junctions is studded with ribosomes (R). (D) A peripheral coupling on the upper surface of a transversely sectioned 3-d myotube. Two feet can be clearly seen (arrowheads). Bar, 10 μm (A and B); 0.2 μm (C and D).

formation and maintenance of the T-tubule/SR junctions is still controversial. Whereas the structural organization of DHPR and RyR (Block *et al.*, 1988) and their coordinated appearance during development are consistent with this idea, as of now there is little direct evidence for such DHPR/RyR interactions. To the contrary, it appears that in skeletal muscle of the dysgenic mouse, which has a deficiency in the DHPR α_1 subunit gene, junctions and RyR clusters can still form in the absence of the DHPR (Pincon-Raymond *et al.*, 1985; Franzini-Armstrong *et al.*, 1991; Flucher *et al.*, 1993b).

The regular arrangement of the triads in the sarcomeres of mature muscle suggests the possibility for an involvement of the myofibrillar apparatus in the development of the E-C coupling membranes. It has been shown that the SR forms early associations with the Z-lines and the I-band region of the myofibrils (reviewed in Flucher, 1992). However, the formation of junctions between the SR and T-tubules as well as the molecular and structural differentiation of their junctional membranes occurs distantly and probably independently from the myofibrils. Interestingly, whereas the junctions without apparent association to myofibrils are heterogeneous in type and shape (diads, inverted triads, standard triads, and multiple junctions), the standard triads are preferentially associated with myofibrils in the more mature myotubes. This could indicate an ordering influence of the myofibrillar apparatus on membrane configuration of the triad. The final step in the organization of the triad is its transverse orientation at the A-I border of the sarcomere. Franzini-Armstrong (1991) reported that in developing mouse muscle fibers this rearrangement involves the whole triad rather than undifferentiated T-tubules. This finding is consistent with the idea that specific interactions between the A-I border region of the myofibrils and the T-tubule/SR junction are responsible for the mature orientation of the triad in the sarcomere. The same mechanism may play a role in the determination of the mature configuration of the triad.

A small population of myotubes in young rat muscle cultures forms junctions between the SR and the plasma membrane. Similar peripheral couplings are expressed transiently during development of skeletal muscle and permanently in atrial muscle and some invertebrate skeletal muscles (Kelly, 1971; Sommer and Waugh, 1976, Hoyle, 1983; Takekura *et al.*, 1993). Although in developing chicken muscle and in rat intercostal muscle in vivo expression of peripheral couplings represents a distinct stage that precedes T-tubule formation, cultured rat myotubes need not form peripheral couplings before T-tubule/SR junctions are established. The peripheral couplings reacted with the antibodies specific for the skeletal isoforms of the DHPR and the RyR. Therefore these couplings resemble T-tubule/SR junctions not only structurally but also in their molecular composition. Furthermore, in young cultures we found no evidence

for two functionally distinct populations of myotubes that would correspond to those containing peripheral couplings or internal junctions. This suggests that calcium release properties of peripheral couplings and T-tubule/SR junctions are essentially the same.

How do the molecular and structural changes that occur during triad formation affect E-C coupling function? Expression of DHPR/RyR clusters and the ability of a myotube to respond to electrical stimulation with calcium release develop concomitantly. Consequently, even the small number of clusters found in newly formed myotubes is capable of sustaining E-C coupling. Many of these young myotubes do not show visible twitches during the calcium transients, suggesting that the myofibrils are not yet sufficiently developed to cause a sizable contraction (Grouselle *et al.*, 1991) or that the distance between the junctions and the myofibrils does not allow an effective activation of the contractile machinery. The functional properties of action potential-induced calcium transients in myotubes are highly variable in young cultures but become increasingly uniform during development. Formation of new myotubes continues over a period of several days. Thus, young cultures consist of myotubes of different developmental stages, explaining the heterogeneity of their calcium transients. One week after replating, formation of new myotubes is complete, and the number of myotubes with immature E-C coupling properties begins to decline. At 10 d after replating, most myotubes display mature characteristics. Contractile activity contributes to the rate of differentiation so that spontaneously active myotubes develop faster than inactive myotubes (Flucher, unpublished data). Because some, mostly isolated, myotubes remain inactive throughout development, some less differentiated myotubes are still present in 10-d-old cultures. The earliest recordings of calcium transients with mature characteristics are from 7-d-old cultures, indicating that the maturation of E-C coupling takes at least 1 wk.

During this period the properties of the action potential-induced calcium transients change in a characteristic way: the rates of the upstroke and of the decay increase, as does the peak amplitude of cytoplasmic free calcium. Although all of these changes occur simultaneously, their development does not seem to be coordinated. Myotubes with fast upstrokes do not necessarily reach high peaks and visa versa. Neither is there a direct relationship between the time constant of the exponential decay and the amplitude or rate of the upstroke. Thus, the development of the release apparatus, the storage capacity, and the reuptake system for calcium proceed independently during myogenesis. Because the Ca^{2+}-ATPase occupies the longitudinal (extrajunctional) SR, a correlation with the junctional release and storage apparatus is not necessarily to be expected. The developmental increase in the density of the Ca^{2+}-ATPase (MacLennan *et al.*, 1985) and in the abundance of longitudinal SR (such as we have observed) could account for the increased uptake rates. However, calcium release rates and storage capacity are both functions of junctional SR and thus should both be directly related to the increase of junction density in the cytoplasm.

The rate of calcium release from the SR in response to an action potential is the parameter most closely related to the formation of functional junctions. The slope of the upstroke is essentially a function of the release rate minus binding of calcium by cytoplasmic buffers and its reuptake by the SR Ca^{2+}-ATPase. Assuming that the rates of calcium binding and reuptake do not diminish during development, the increased slope of the upstroke reflects an actual increase in calcium release rates. This marked developmental increase of release rates may be primarily accomplished by the continuous formation of new junctions. In addition, myofibrils and membranous compartments occupy an increasing portion of the cytoplasm. Thus, the ratio of total junction area versus free cytoplasm may increase dramatically, contributing to the sharp rise in cytoplasmic free calcium upon E-C coupling in fast twitch fibers. The regular distribution of the junctions in the sarcomeres may further add to the efficient rise and removal of cytoplasmic calcium throughout the myotube.

The combined analysis of Ca^{2+} release properties and the molecular and structural differentiation of the release apparatus shows that the basic function of E-C coupling in skeletal myotubes develops upon formation of peripheral couplings and T-tubule/SR junctions. In contrast, the maturation of E-C coupling properties may be a function of the increasing density and redistribution of junctions in the cytoplasm. The mechanism of junction formation is closely linked to the molecular specialization of the participating membrane domains, yet appears not to require direct interactions between the DHPR and the RyR. The reorganization of the junctions into proper triads occurs only secondarily and is closely tied to their association to the myofibrils at the A-I border of the sarcomere.

ACKNOWLEDGMENTS

We thank Drs. S. Fleischer and S. Froehner for generously supplying the antibodies for this study. We also thank C. Mueller for help with cell cultures and electron microscopic preparation, E.D. Foster for morphometry, and W. Rasband for his support with the Image software.

REFERENCES

Block, B.A., Imagawa, T., Campbell, K.P., and Franzini-Armstrong, C. (1988). Structural evidence for direct interaction between the molecular components of the transverse tubule/sarcoplasmic reticulum junction in skeletal muscle. J. Cell Biol. *107*, 2587–2600.

Daniels, M.P. (1990). Localization of actin, β-spectrin, 43×10^3 M_r and 58×10^3 M_r proteins to receptor-enriched domains of newly formed acetylcholine receptor aggregates in isolated myotube membranes. J. Cell Sci. *97*, 615–627.

Eusebi, F., Miledi, R., and Takahashi, T. (1980). Calcium transients in mammalian muscles. Nature *284*, 460–561.

Flucher, B.E. (1992). Structural analysis of muscle development: transverse tubules, sarcoplasmic reticulum and the triad. Dev. Biol. *154*, 245–260.

Flucher, B.E., and Andrews, S.B. (1993). Characterization of spontaneous and action potential-induced calcium transients in developing myotubes in vitro. Cell Motil. Cytoskeleton *25*, 143–157.

Flucher, B.E., Andrews, S.B., Fleischer, S., Marks, A.R., Caswell, A., and Powell, J.A. (1993a). Triad formation: organization and function of the SR calcium release channel and triadin in normal and dysgenic muscle in vitro. J. Cell Biol. *123*, 1161–1174.

Flucher, B.E., Morton, M.E., Froehner, S.C., and Daniels, M.P. (1990). Localization of the α_1 and α_2 subunits of the dihydropyridine receptor and ankyrin in skeletal muscle triads. Neuron *5*, 339–351.

Flucher, B.E., Phillips, J.L., and Powell, J.A. (1991a). Dihydropyridine receptor α subunits in normal and dysgenic muscle in vitro: expression of α_1 is required for proper targeting and distribution of α_2. J. Cell Biol. *115*, 1345–1356.

Flucher, B.E., Phillips, J.L., Powell, J.A., Andrews, S.B., and Daniels, M.P. (1992). Coordinated development of myofibrils, sarcoplasmic reticulum and transverse tubules in normal and dysgenic mouse skeletal muscle, in vivo and in vitro. Dev. Biol. *155*, 266–280.

Flucher, B.E., Takekura, H., and Franzini-Armstrong, C. (1993b). Development of the excitation-contraction coupling apparatus in skeletal muscle: association of sarcoplasmic reticulum and transverse tubules with myofibrils. Dev. Biol. *160*, 135–147.

Flucher, B.E., Terasaki, M., Chin, H., Beeler, T., and Daniels, M.P. (1991b). Biogenesis of transverse tubules in skeletal muscle in vitro. Dev. Biol. *145*, 77–90.

Fosset, M., Jaimovich, E., Delpont, E., and Lazdunski, M. (1983). [3H]nitrendipine receptors in skeletal muscle: properties and preferential localization in transverse tubules. J. Biol. Chem. *258*, 6086–6092.

Franzini-Armstrong, C. (1970). Studies of the triad. I. Structure of the junction in frog twitch fibers. J. Cell Biol. *47*, 488–499.

Franzini-Armstrong, C. (1991). Simultaneous maturation of transverse tubules and sarcoplasmic reticulum during muscle differentiation in the mouse. Dev. Biol. *146*, 353–363.

Franzini-Armstrong, C., Pinçon-Raymond, M., and Rieger, F. (1991). Muscle fibers from dysgenic mouse in vivo lack a surface component of peripheral couplings. Dev. Biol. *146*, 364–376.

Grouselle, M., Koenig, J., Lascomb, L.-M., Chapron, J., Méléard, P., and Georgescauld, D. (1991). Fura-2 imaging of spontaneous and electrically induced oscillations of intracellular free Ca^{2+} in rat myotubes. Pflügers Arch. *418*, 40–50.

Hoyle, G. (1983). Forms of modulatable tension in skeletal muscles. Comp. Biochem. Physiol. [A] *76*, 203–210.

Inui, M., Saito, A., and Fleischer, S. (1987). Purification of the ryanodine receptor and identity with feet structures of junctional terminal cisternae of sarcoplasmic reticulum from fast skeletal muscle. J. Biol. Chem. *262*, 1740–1747.

Ishikawa, H. (1968). Formation of elaborate networks of T-system tubules in cultured skeletal muscle with special reference to the T-system formation. J. Cell Biol. *38*, 51–66.

Jorgensen, A.O., Shen, A.C., Arnold, W., Leung, A.T., and Campbell, K.P. (1989). Subcellular distribution of the 1,4-dihydropyridine receptor in rabbit skeletal muscle in situ: an immunofluorescence and immunocolloidal gold-labeling study. J. Cell Biol. *109*, 135–147.

Kelly, A.M. (1971). Sarcoplasmic reticulum and T tubules in differentiating rat skeletal muscle. J. Cell Biol. *49*, 335–344.

Lai, F.A., Erickson, H.P., Rousseau, E., Liu, Q.Y., and Meissner, G. (1988). Purification and reconstitution of the calcium release channel from skeletal muscle. Nature *331*, 315–319.

MacLennan, D.H., Zubryzycka-Gaarn, E., and Jorgensen, A.O. (1985). Assembly of the sarcoplasmic reticulum during muscle development. In: Current Topics in Membranes and Transport, vol. 24, ed. F. Bronner, New York: Academic Press, 337–368.

Morton, M.E., and Froehner, S.C. (1987). Monoclonal antibody identifies a 200-kD α subunit of the dihydropyridine-sensitive calcium channel. J. Biol. Chem. *262*, 11904–11907.

Olek, A.J., Ling, A., and Daniels, M.P. (1986). Development of ultrastructural specializations during the formation of acetylcholine receptor aggregates on cultured myotubes. J. Neurosci. *6*, 487–497.

Peachey, L.P., and Franzini-Armstrong, C. (1983). Structure and function of membrane systems of skeletal muscle cells. In: Handbook of Physiology: Section 10, Skeletal Muscle, eds. L.D. Peachey, R.H. Adrian, and S.R. Geiger, Bethesda, MD: American Physiological Society, 23–71.

Pinçon-Raymond, M., Garcia, L., Romay, G., Lazdunski, M., and Rieger, F. (1990). A genetic model for the study of abnormal nerve-muscle interactions at the level of excitation-contraction coupling: the mutation muscular dysgenesis. J. Physiol. *84*, 82–87.

Rios, E., and Brum, G. (1987). Involvement of dihydropyridine receptors in excitation-contraction coupling in skeletal muscle. Nature *325*, 717–720.

Rüegg, J.C. (1988). Calcium in muscle activation. Berlin: Springer Verlag.

Schiaffino, S., Cantini, M., and Sartore, S. (1977). T-system formation in cultured rat skeletal tissue. Tissue & Cell *9*, 437–446.

Sommer, J.R., and Waugh, R.A. (1976). The ultrastructure of the mammalian cardiac muscle cell—with special emphasis on the tubular membrane systems. A review. Am. J. Pathol. *82*, 192–232.

Striessnig, J., Moosburger, K., Goll, A., Ferry, D., and Glossmann, H. (1986). Stereoselective photoaffinity labeling of the purified 1,4-dihydropyridine receptor of the voltage-dependent calcium channel. Eur. J. Biochem. *161*, 603–609.

Takekura, H., Shuman, H., and Franzini-Armstrong, C. (1993). Differentiation of membrane systems during development of slow and fast skeletal muscle fibres in chicken. J. Muscle Res. Cell Motil. *14*, 633–45.

Wagenknecht, T., Grassucci, R., Frank, J., Saito, A., Inui, M., and Fleischer, S. (1989). Three-dimensional architecture of the calcium channel/foot structure of sarcoplasmic reticulum. Nature *338*, 167–170.

Yuan, S., Arnold, W., and Jorgensen, A.O. (1990). Biogenesis of transverse tubules: immunocytochemical localization of a transverse tubular protein (TS28) and a sarcolemmal protein (SL50) in rabbit skeletal muscle in situ. J. Cell Biol. *110*, 1187–1198.

Yuan, S., Arnold, W., and Jorgensen, A.O. (1991). Biogenesis of transverse tubules and triads: immunolocalization of the 1,4-dihydropyridine receptor, TS28, and the ryanodine receptor in rabbit skeletal muscle developing in situ. J. Cell Biol. *112*, 289–301.